Molecular Quantum Cellular Automata Cell Design Trade-offs: Latching vs Power Dissipation

Ehsan Rahimi[a] and Jeffrey R. Reimers[bc]

Use of molecules to enact quantum cellular automata (QCA) cells has been proposed as a new way for performing electronic logic operations at sub-nm dimension. A key question that arises concerns whether chemical or physical processes are to be exploited. Use of chemical reactions allows the state of a switch element to be latched in molecular form, making the output of a cell independent of its inputs, but costs energy to do the reaction. Alternatively, if purely electronic polarization is manipulated then no internal latching occurs but no power is dissipated provided the fields from the inputs change slowly compared to the molecular response times. How these scenarios pan out is discussed by considering calculated properties of the 1,4-diallylbutane cation, a species often used as a paradigm for molecular electronic switching. Utilized are results from different calculation approaches that depict the ion, either as a charge-localized mixed-valence compound functioning as a bistable switch, or else as an extremely polarizable molecule with a delocalized electronic structure. Practical schemes for using molecular cells in QCAs and other devices emerge.

A. Introduction

Reductions in the size and power consumption of electronic transistors has led to a remarkable advance in electronics technology.[1] Molecular switches have been long promoted as possible end-points in this advance,[2, 3] but for them the same scenario of power dissipation can be expected as in CMOS technology, as the electrons directly interact with the contacts and nuclear motion is intrinsically involved in all processes. Even in ballistic electronic devices, power dissipation at the contacts is inevitable. In current silicon electronics, data is stored in flip-flops that process input signals upon a clock pulse, which results in a latched output signal driving a fan-out to many subsequent inputs. This desirable process happens at the expense of the power that is dissipated when the flip-flops change state. Bistable molecules have been proposed as molecular switches that can store charge in isomeric forms for long periods of time without need for external power, but energy is dissipated as heat by the exothermic chemical reactions that change the state of the switch.[4-6]

Quantum-dot cellular automata (QCA) have been proposed as a new technology that promises to break existing paradigms related to power dissipation and contacts.[7-10] Common QCA designs localize two electric charges on 4-6 sites per cell, as sketched in Fig. 1. In a 4-site cell, two patterns are possible, conceived as providing "0" and "1" logic states in a device, with a third "null" state added in a 6-site cell.[11] While single molecules containing all desired functionality can be envisaged, smaller molecules containing each 2 or 3 sites may be assembled together to make a single cell.[11-34]

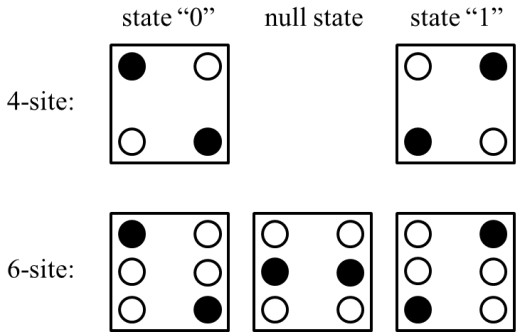

Figure 1. QCA cells contain either 4 or 6 sites into which two charges (filled circles) are stored. The allowed patterns of charge storage depict two binary logic states and, optionally, an intermediary null state.[11]

Independent of the number of sites in a cell and their representations, cell operation involves rearrangement of the charges stored at each site. In a 4-site cell these rearrangements interchange the "0" and "1" states, whereas interchanging of "0" and "null", or "null" and "1", states is usually envisaged in 6-site cells. If these rearrangements can be performed adiabatically by changing applied electric fields slowly compared to the intrinsic response times of the cell components, then the charge rearrangements can be done reversibly without energy penalty.[35] This possibility has led to many anticipated outcomes concerning futuristic electronic devices[35-37] consuming ultra-low power.

If device operation involves only electronic polarization and not nuclear motion, then the adiabatic switching paradigm should be realizable. In large cells like fabricated quantum dots on silicon, moving electrons delocalize over very many atoms and so minimal nuclear motion is associated with their rearrangement. Also, nuclear motion does not intrinsically inhibit adiabatic operation, with nuclear rearrangements of capacitor dielectrics providing an important example of how adiabatic transformations can occur. Slowly varying applied electric fields ever-so-slightly perturb the molecular structure; only when the field is varied at molecular frequencies does the dielectric absorb and dissipate energy.

However, molecular switch operation, including the incorporation of molecular switch units into QCA cells, is

[a] Faculty of Electrical and Robotic Engineering, Shahrood University of Technology, Shahrood, Iran E-mail: erahimi@shahroodut.ac.ir
[b] International Centre for Quantum and Molecular Structures and School of Physics, Shanghai University, Shanghai 200444 China. E-mail: Jeffrey.Reimers@uts.edu.au; Tel: +86-15618155341
[c] School of Mathematical and Physical Sciences, University of Technology Sydney, NSW 2007 Australia.
Electronic Supplementary Information (ESI) available: Optimized atomic coordinates, energies, etc.].

usually discussed in terms of the manipulation of bistable chemical reactions.[3, 6, 10, 11, 15, 19, 22, 38] In these, small changes in external conditions facilitate the reaction at some critical applied field strength, producing fs-timescale nuclear motions that dissipate heat in an irreversible fashion.[6, 39, 40] Hence the adiabatic switching paradigm does not apply to bistable molecular switches. Applied to QCA's, this means that power is dissipated whenever a cell changes between any of its possible "0", "null", or "1" states.

The operation of bistable molecular switches is usually described in terms of adiabatic electron-transfer theory.[4-6, 19, 20, 39, 41-52] This is a wide ranging approach that not only describes electrochemical reactions at electrodes, biological electron transfer, organic conductors and organic solar cells, but also phenomena such as quantum tunnelling and decoherence[53, 54] as well as quantum entanglement[52] and quantum computing applications.[55] Its origins involve the explanation of the nature and spectroscopy of mixed-valence molecules and complexes[39] that can adopt two or more electronic configurations. All bistable molecular switches that have been proposed for use in electronics are examples of such species.

Critical elements of adiabatic electron-transfer theory are sketched in Fig. 2. A molecule or molecular assembly is categorized into two parts, A and B, each of which may take different charges; here for convenience we depict species A^+B and AB^+. Each species has a different equilibrium geometry and is attributed a harmonic diabatic potential-energy surface in some generalized coordinate that interchanges these geometries. The energy associated with the geometry change is the reorganization energy λ, while the resonance energy coupling the diabatic states is J; $E_0(F)$ is the equilibrium energy difference, here taken as a function of some externally controllable electric field of strength F. Application of the Born-Oppenheimer approximation to the model leads to adiabatic ground-state and excited-state potential-energy surfaces, with the actual charge on each species varying continuously during the electron-transfer process.[5, 56, 57] Two distinct scenarios arise depending on whether or not the ground-state surface shows a double-minimum. When $E_0(F) = 0$, (i.e., for a symmetric reaction), this occurs whenever $2|J|/\lambda < 1$,[44, 58] with the general condition also being known[57] and interrelationships described.[59] When a double-minimum exists and is sufficiently deep to support zero-point vibration in each well,[60] charge-localized isomers can be identified, defining the states of a bistable switch. This scenario is sketched in Fig. 2a. Absence of a double minimum can indicate either the inverted region[4, 58, 61] ($|E_0(F)|>\lambda$ as $J\rightarrow 0$), or the delocalized region[39, 58] in which only one isomer can be isolated with charge distributed roughly equally between A and B, as sketched in Fig. 2b. The inverted region also depicts a bistable switch, but all reactions proceed very slowly by quantum tunnelling and dissipate large amounts of heat,[4, 40, 42, 62] features not appropriate for molecular switch and QCA operation. However, the delocalized regime is fundamentally different, with only one stable state of the system.

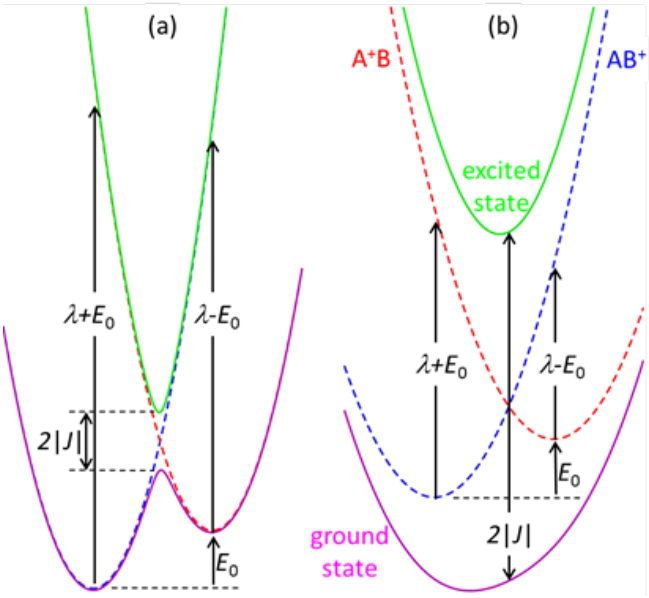

Fig. 2. Scenarios for mixed-valence compounds from adiabatic electron-transfer theory: (a) localized case forming a bistable molecular switch with $2J/\lambda=1/8$, $E_0/\lambda=1/8$, and (b): delocalized case forming a highly polarizable dielectric with $2J/\lambda=3/2$, $E_0/\lambda=1/4$. The curves depict energy as a function of a generalized reaction coordinate converting A^+B into AB^+; J is the resonance energy, λ the reorganization energy, and E_0 the electric-field dependent difference in localized-state energies. Blue and red dashed curves are diabatic surfaces representing A^+B into AB^+ while magenta and green solid curves are the resulting Born-Oppenheimer adiabatic potential-energy surfaces.

In this work, we consider calculated properties of the 1,4-diallylbutane cation (Fig. 3), a long molecule with sites at each end that can take on either the positive charge or else a free radical. This system has historically been used as a paradigm for molecular switch operation.[3, 6, 10] Spin-unrestricted Hartree-Fock (UHF) theory predicts this molecule in the gas phase to have the charge/spin in one of the localized states depicted in Fig. 3 and is hence a bistable switch describable based on Fig. 2a in terms of classical isomerization chemistry. However, we show that higher levels of theory predict it to be a charge/spin delocalized (resonant-hybrid) system describable instead by Fig. 2b.

Delocalized mixed-valence molecules are extremely polarizable,[47, 63] a feature that in itself can be exploited for QCA operation. While polarization does involves nuclear motion to some degree, there is no chemical reaction involved and so the nuclear motion occurs adiabatically, similar to the reorientational motions of the material in a capacitor that give rise to its high static dielectric constant. Hence delocalized mixed-valence molecules offer a route to the dream of ultra-low power circuit operation.

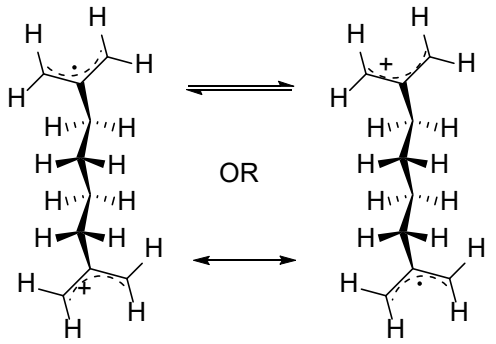

Figure 3. The 1,4-diallylbutane cation $[(C_3H_4)CH_2CH_2CH_2CH_2(C_3H_4)]^+$ can be represented as two forms with spins and charges localized on opposite ends of the molecule. These structures may either be isolable chemical species with charge/spin localized structures displaying valence tautomerization (see Fig. 2a), or else exist as a single resonance hybrid (see Fig. 2b) with the charge and spin equally delocalized over both ends. Either two or three of these molecules must be self-assembled to make a QCA cell (see Fig. 1).

In any practical application of molecular switches in QCAs or other circuitry, environmental factors will significantly affect intrinsic gas-phase molecular properties, generating many chemical scenarios and/or details.[51] Such practicality is not our concern here. Instead, the availability of two different computational scenarios for the 1,4-diallylbutane cation is used to facilitate understanding of generic properties of bistable and monostable molecular electronic components. In each case, we predict key operational properties including: power dissipation, reversible energy storage and release, maximum switching frequency, and latching lifetime.

Optimization of QCA performance involves a trade-off between minimizing power dissipation and maximizing functionality. Any component that runs based on slow adiabatic processes does not, within itself, provide latching of the state of the device, meaning that "inputs" and "outputs" are fundamentally the same, with any variation at an "output" being able to reverse-drive devices connected to the related "inputs". No practical large-scale device can be operated this way. An engineering solution to this problem is to connect some of the "inputs" in a complex cell to external clocking busses that themselves consume power, but are robust enough to latch the state of the "output" independent of variations in the computationally active "logic inputs".[36] On the other hand, bistable molecular switches interconvert isomers that have their own intrinsic stability, isolating "outputs" from "inputs" to latch states. However, the power that bistable switches consume still needs to be provided to each cell in a device, for which again external clocking provides an engineering solution. At the single-switch level, the key questions therefore become: how much power does a bistable switch need to function, and how functional can a monostable component be?

B. Properties of the 1,4-diallylbutane cation

In 1,4-diallylbutane, charges and spins distribute mostly amongst the allyl π orbitals. At the symmetric charge/spin delocalized C_{2h} geometry of the cation, these orbitals are shown in Fig. 4. The functional π groups at the end of the molecule are characterized each by three orbitals: a low-energy bonding orbital, a mid-energy non-bonding orbital, and a high-energy antibonding orbital. In the molecule these six localized orbitals are free to interact, with the resulting molecular orbitals shown in the figure. In the cation of 1,4-diallylbutane, all bonding orbitals are doubly occupied whilst one electron total is placed into the two non-bonding orbitals.

As the allyl groups are oriented perpendicular to the plane of the alkyl chain, the allyl π orbitals can mix with the chain σ orbitals, as is apparent from Fig. 4. Strong mixing is found between the π-bonding orbital pair but very weak mixing occurs for the non-bonding orbital pair as by symmetry they have zero coefficients on the bridgehead carbons and hence interact only weakly with the intervening C-C σ bonds. Hence the resonance energy *J* coupling these orbitals is very small.

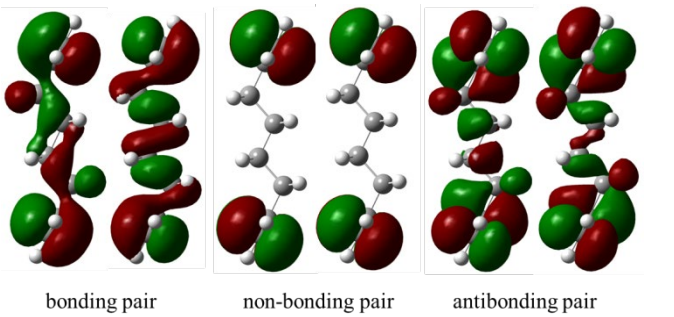

Figure 4. The six allyl-π dominated molecular orbitals of 1,4-diallylbutane, evaluated using B3LYP/6-31G* at the C_{2h} structure of the neutral closed-shell species.

Situations in which the direct coupling between key orbitals is large are usually easy to understand. However, when *J* is near zero, superexchange interactions coupling the orbitals of interest through other orbitals becomes critical. Such effects are an aspect of *dynamic electron correlation*. Also, another significant issue for the 1,4-diallylbutane cation is that real wavefunctions must display the global symmetry properties of the molecule (as those in Fig. 4 do), but slight asymmetry in the geometry generates immediate orbital localization, breaking symmetry. This effect is called *static electron correlation*. Accurate results for 1,4-diallylbutane require proper treatment of both effects.

In iconic studies of the 1,4-diallylbutane cation, the UHF computational method has been used, mostly with minimal basis sets like STO-3G. These predict charge-localized bistable structures of C_s or lower symmetry (Fig. 2a, Fig. 3).[3, 6, 10] A significant feature of UHF calculations not previously stressed is that they induce spontaneous symmetry breaking, making the symmetry of the electronic wavefunction lower than that of the nuclei, an unphysical solution. UHF optimized structures in which both the electronic and nuclear symmetries are constrained to either C_{2h} symmetry are listed in Electronic Supporting Information (ESI) and are higher in energy by 1.1 eV compared to their symmetry-broken counterparts. Also, the C_{2h} structure is characterized by vibrational frequency analysis as a local-minimum on the potential-energy surface.

One significant anomalous feature associated with the symmetry breaking of UHF solutions is that the ground-state wavefunction, and hence all properties such as calculated dipole moment, changes discontinuously as the C_{2h} geometry is crossed. This feature is unphysical but has been utilized in previous analyses of QCA operation.[10] Recent calculations using semi-empirical implementations of density-functional theory do not reproduce this effect.[19]

Complete active space self-consistent field (CASSCF) theory in principle provides a means for dealing with these issues as it explicitly includes static electron correlation. Naively the two allyl open-shell orbitals would be expected to be of greatest importance and hence calculations treating exactly one electron distributed in these two orbitals, termed "CASSCF(1,2)", should be sufficient. However, we find that symmetry breaking remains a feature of such CASSCF calculations (using the 6-31G* basis set), but the potential-energy surfaces do become continuous. Also, the twisting of the allyl group originally observed in UHF calculations is maintained, as naively expected, see ESI for details. While CASSCF presents a significant improvement to UHF theory, it still does not include dynamic electron correlation, an effect that could seriously modify the perceived electronic coupling, J and reorganization energy, λ.

Three computational methods are used that do include dynamic electron correlation: the B3LYP and CAM-B3LYP methods from density-functional theory (DFT) and the multi-reference configuration interaction (MRCI) approach based on a CASSCF(1,2) initial wavefunction. These methods may or may not include enough static electron correlation to produce continuous potential-energy surfaces, but for the 1,4-diallylbutane we find that indeed continuous surfaces are obtained. Significantly, they all predict that the 1,4-diallylbutane cation has a single minimum at a charge/spin delocalized C_{2h} structure akin to Fig. 2b. Dynamic electron correlation hence enhances $2|J|/\lambda$, indicating very different operation of this species in a molecular device.

Concerning these calculations, two features should be noted. First, all geometry optimizations reported in ESI were obtained using B3LYP, with CAM-B3LYP and MRCI energies and other properties evaluated at these geometries. Second, not all issues regarding static electron correlation are solved by DFT calculations, with for example time-dependent density-functional theory (TDDFT) being difficult to apply owing to its singlet-triplet instability and related problems.[64] This issue is particularly relevant in the modern context of DFT and TDDFT applications to the study of defect sites in 2D materials,[65] presenting many aspects pertinent to molecular switch design.

C. The 1,4-diallylbutane cation as a paradigm for QCA function using delocalized mixed-valence molecules

In this section, we consider the 1,4-diallylbutane cation, as perceived by the B3LYP, CAM-B3LYP, and MRCI methods, as a delocalized mixed-valence molecule. At high-symmetry C_{2h} geometries, B3LYP, CAM-B3LYP, and MRCI predict the ground state to be ^2A_u, with a transition energy to the nearly degenerate ^2B_g state being at energies of 0.014 eV (B3LYP), 0.016 eV (CAM-B3LYP) or 0.035 eV (MRCI). These numbers are estimates of $2|J|$, so the resonance energy remains low, even after dynamical electron correlation is included. The reorganization energy must be even lower, however, as $2|J|/\lambda>1$ for delocalized ground states.

One of the most significant properties of a delocalized mixed-valence system is its electronic polarizability, α. This is a tensor quantity, but here we consider only its component in the critical allyl-allyl direction. Normal intuition concerning the properties of polarizability come from the assumption that the ground-state is non-degenerate, leading to[63]

$$\alpha = \sum_i \frac{2M_i^2}{h\nu_i} \qquad (1)$$

where M_i is the appropriate component of the transition dipole vector facilitating optical excitation to state i at energy $h\nu_i$. Adiabatic electron-transfer theory recognizes that, in charge-transfer systems, the dominant contribution to this sum comes from the intervalence charge-transfer band,[39, 63] here the low-energy $^2A_u \rightarrow {}^2B_g$ excitation. For this, the expected transition moment is $M \sim R/2$ ~ 3.8 eÅ where R is the allyl-allyl separation, quite a large number. However, as $h\nu$ is near zero, Eqn. (1) greatly overestimates the actual polarizability.

Indeed, CASSCF and MRCI both predict the transition moment of the intervalence band to be near 3.8 eÅ in accordance with expectations. However, B3LYP predicts 0.85 eÅ whilst CAM-B3LYP predicts 1.20 eÅ. In parallel, the actual polarizability calculated directly by B3LYP of 102 Å^3 increases to 350 Å^3 for CAM-B3LYP. CAM-B3LYP pushes up charge-transfer transition energies to lower polarizabilities, eliminating catastrophic problems found when methods like B3LYP and simpler functionals are applied to systems with extended conjugation such as aromatic chromophores and polyacetylene.[66, 67] For the 1,4-diallylbutadiene cation, counterintuitively CAM-B3LYP significantly increases the transition moment and polarizability. Conversely, MRCI predicts M = 3.8 eÅ but a polarizability of only 93 Å^3, indicating the failure of Eqn. (1) and the great sensitivity of QCA properties to the computational method used.

Exploiting the similarities between B3LYP and MRCI results, B3LYP is used to characterize the response properties of the 1,4-diallylbutane cation to an applied electric field in the allyl-allyl direction of magnitude F, with results given in Table 1. First, the field is applied to a molecular structure frozen at the equilibrium C_{2h} geometry of the field-free molecule, the change in energy $\Delta E(F)$ and induced dipole moment $\mu(F)$. All

Table 1. Calculated properties of the cation of 1,4-diallylbutane as a function of an external field applied in the end-to-end direction.

F		C_{2h} geometry[a]		C_s geometry[b]					
		$\Delta E(F)$	$\mu(F)$	$\Delta E(F)$	$\mu(F)$	$\Delta E(0)$[c]	$\mu(0)$[c]	$\bar{\nu}$	τ
au	VÅ^{-1}	eV	eÅ	eV	eÅ	eV	eÅ	cm^{-1}	fs
0	0.000	0.000	0.0	0.000	0.4	0.000	-0.03	-	-
0.001	0.051	-0.009	0.4	-0.010	0.8	0.000	-0.05	920	36
0.002	0.103	-0.037	0.7	-0.040	1.2	0.002	-0.08	686	49
0.003	0.154	-0.084	1.1	-0.090	1.6	0.005	-0.10	524	64
0.004	0.206	-0.150	1.5	-0.160	2.0	0.010	-0.13	434	77
0.005	0.257	-0.234	1.8	-0.251	2.4	0.017	-0.15	384	87
0.006	0.309	-0.337	2.2	-0.362	2.8	0.025	-0.18	358	93
0.007	0.360	-0.458	2.5	-0.494	3.2	0.035	-0.20	346	96
0.008	0.411	-0.598	2.9	-0.647	3.6	0.048	-0.23	340	98
0.009	0.463	-0.757	3.3	-0.820	3.7	0.062	-0.24	337	99
0.01	0.514			-1.008		0.072		327	102

a: The external field is applied but the geometry is constrained to the field-free high-symmetry charge delocalized geometry.

b: The geometry used corresponds to that optimized in the presence of the external field.

c: The notation "(0)" indicates that the geometries used were optimized in the presence of the field but the properties are evaluated with the field removed.

results indicate an electronic polarizability of 102 Å^3. At a field strength of 0.01 au (0.51 VÅ^{-1}), charge separation is induced in the molecule as if a bistable switch was activated and the charge localized on one of the allyl groups. A field of this magnitude is very large but not atypical of the field coming from localized nearby ions. In practical terms, one would need to trade off the need for a large dielectric constant to stabilize the molecular charge and a small dielectric constant to support such high field strengths. Nevertheless, we see that a delocalized system can in principle still support basic QCA functionality, without the need for a heat-producing chemical reaction to induce large charge fluctuations

Next, Table 1 shows the results of optimizing the nuclear geometry in the presence of the field. The induced changes in $\Delta E(F)$ and $\mu(F)$ are only small. Finally, Table 1 shows the energy change $\Delta E(0)$ and dipole change $\mu(0)$ of the ion in the absence of an applied field at the geometry optimized in the presence of the field, again realizing only small changes. Both sets of results indicate that electronic polarization rather than nuclear polarization is the primary effect in operation when the 1,4-diallylbutane cation is exposed to an electric field. Nevertheless, $\Delta E(0)$ indicates the energy associated with nuclear polarization stored adiabatically as molecular potential energy as the field strength increases. When the applied field is removed, this energy is returned into the system without associated energy dissipation as heat.

D. The 1,4-diallylbutane cation as a paradigm for QCA function using localized mixed-valence molecules

Discussion in previous decades[3, 6, 10] featuring the 1,4-diallyl cation as a paradigm for molecular switches and its usefulness in QCA operation has been based on UHF results that seemingly incorrectly predict the ion to support charge-localized structures typical of a bistable switch (Figs. 2a and 3). However, continued discussion of these results remains useful as basic generic principles are easy to demonstrate and understand.[6] The effect of applied electric fields on the adiabatic potential-energy surfaces predicted at the UHF/STO-3G level is shown in Fig. 5. The nuclear coordinate used in this figure is obtained by linear interpolation between optimized C_{2h} and C_s structures.

In the absence of an applied field, the diabatic potential energy surfaces depicting charge-localized states intersect at the C_{2h} geometry, experiencing almost no coupling. If a harmonic approximation to the shapes of these surfaces is introduced, then the energy difference between this point and the C_s minima of 0.062 eV is interpreted as being $\lambda/4$.[4, 5]

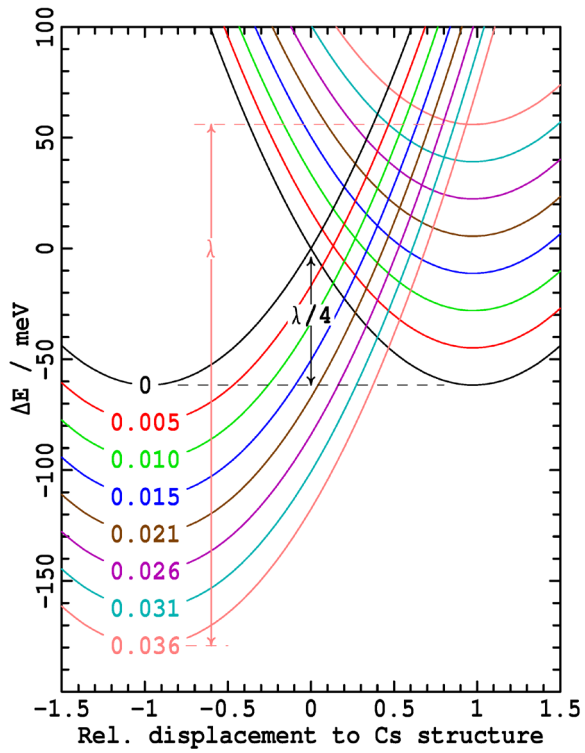

Figure 5. Operation of the 1,4-diallylbutate cation as a bistable switch as predicted by UHF/STO-3G, displaying charge/spin localized molecular potential-energy surfaces for different applied electric field strengths (in VÅ^{-1}) as a function of a coordinate that linearly interpolates between the optimized C_{2h} and C_s molecular structures. λ is the associated reorganization energy which is immediately dissipated as heat through intramolecular vibrational relaxation once the critical field strength of 0.036 VÅ^{-1} is reached, latching the switch in its new state.

Applied electric fields in the inter-allyl direction are then applied with increasing magnitude, causing the relative energies of the localized surfaces to alternatively increase or decrease. We take the charge to be initially localized in the right-hand well, the field acting to destabilize this state compared to that in which the charge localizes in the left-hand well. If the field is changed slowly enough, the molecule responds adiabatically with no power dissipated. Ignoring the effects of quantum tunnelling,[5, 40] this situation continues until the critical field strength[6] of $F = \Delta\mu/\lambda = 0.036$ VÅ^{-1} is reached. Then, the left-hand surface crosses the right-hand one at its equilibrium geometry and a classical chemical reaction ensures that change the state of the switch, liberating $\lambda = 0.24$ eV energy as heat, on the fs timescale, through intramolecular and intermolecular vibrational relaxation.

Operating under classical chemical principles, the minimum amount of energy that is released as heat during the electron-transfer reaction is therefore the reorganization energy λ.[5, 6, 39] Historically, interpretations of QCA properties[10] have ignored this effect, leading to unrealistic descriptions of QCA functionality. The amount of energy liberated when a bistable chemical switch changes state could be reduced if tunnelling promoted the electron transfer at lower applied field strengths,[9,45,59] provided the tunnelling rate being is much faster than the rate at which the applied field is changed. A pertinent example of this effect is presented in the recent quantum simulations of molecular-switch operation of Blair, Corcelli, and Lent.[40] In this, $\lambda/4 \sim 3h\nu$ with the tunnelling involving exchange of 2 vibrational quanta, reducing the energy dissipation to ~ λ/5, close to the optimal case for heat reduction (see Figs. 17 and 18 in ref.[40]). This process is not likely for the 1,4-diallylbutane cation as there is essentially no electronic coupling to drive it,[42, 57, 62] but in general it is an expected process and its likely consequences concerning latching are considered in the next Section.

E. The timescale for nuclear motion, estimated device power consumption, tunnelling effects and the latching trade-off

Regardless of whether or not a mixed valence molecule used in a QCA context is bistable, the timescale for nuclear motion provides an important system parameter. If the applied electric field changes on this timescale then the molecular system will resonantly absorb power from the oscillating field. Decoherence of such driven nuclear motion by intramolecular vibrational relaxation would be very difficult to prevent and therefore the process would necessarily result in energy loss by heating. If the field changes faster than the nuclear vibrations can respond then nuclear excitation will decrease, but optical excitation will commence instead. The desired scenario is therefore for the field to change slowly compared to vibrational response times, enabling adiabatic switching effects to minimize power dissipation. Tunnelling effects also act to minimize power dissipation in this scenario.

The field-dependent timescale for the nuclear motion in the 1,4-diallylbutane cation that moves charge from one end of the molecule to the other is estimated in Table 1 based on B3LYP calculations. To do this, the displacements calculated at field strength *F* are projected onto the normal vibrational modes of the molecular cation at its equilibrium C_{2h} geometry, evaluating the average frequency

$$\bar{\nu} = \frac{\frac{1}{2}\sum_i \nu_i \delta_i^2}{\frac{1}{2}\sum_i \delta_i^2} = \frac{\lambda}{S} \qquad (2)$$

where ν_i are the harmonic vibration frequencies, δ_i are the mode displacements in zero-point ($\hbar^{1/2} / \omega^{1/2}$) units,[68, 69] and *S* is the Huang-Rhys factor. This average frequency changes from 920 cm^{-1} at low field strengths to 327 cm^{-1} at large values as a result of multiple chemical effects contributing to charge separation. The inverse of the average frequency is the minimum time τ required to switch the nuclear polarization: 100 fs at anticipated operation field strengths.

If the applied electric field is changed slowly on this 100 fs time scale, then vibrational excitation of the electronically active modes cannot occur. The B3LYP calculations, depicting the 1,4-diallylbutane cation as a delocalized species, then indicate that the adiabatic switching scenario applies and minimal power dissipation as heat is expected. However, if the UHF/STO-3G results pertain, then, neglecting tunnelling, λ =

0.24 eV energy is dissipated as heat per electron switch within each QCA cell in a complex device. If 10^{10} such electrons in a multitude of cells are transferred per cycle in a large integrated circuit running at a frequency of 1 THz, the power dissipation would be 380 W. Of course, not all parts of a large integrated circuit switch every cycle, so this result is consistent with state of the art circuitry requirements. A reorganization energy of this magnitude would latch the output of a cell for a time of about $\overline{\nu}^{-1}e^{-\lambda/4kT}$ or just 1 ps at an operation temperature of T = 340 K, hardly an adequate value. To be useful, the latching time must be such that there is less than a 1 in a 1000 chance that thermal motion destroys the latch within one clock cycle, a feature that on-chip error correcting hardware could effectively deal with. In a logic design based on an internally latched bistable molecular switch, the reorganization energy required to provide this level of accuracy must scale as

$$\lambda = 4kT\ln\left(\frac{7}{\overline{\nu}f}\right) \qquad (3)$$

where f is the intended operation frequency. For a typical nuclear motion time of 10^{-13} s, this requires λ = 0.51 eV, 0.79 eV, and 1.06 eV for operation at 10^{12} Hz, 10^{11} Hz, and 10^{9} Hz, respectively. Interestingly, demands go down as the operation frequency increases.

This analysis is based on the assumption that the device operates through classically allowed chemical reactions unaided by quantum nuclear tunnelling. To guarantee fidelity, the amount of energy liberated as heat does not change and remains $4kT\ln(7/\overline{\nu}f)$. So, as tunnelling reduces heat dissipation in any system below λ, the required reorganization energy must increase to compensate. The net effect is a zero-sum gain situation; basically, if tunnelling can aid the desired process than it similarly aids the reverse reaction, reducing device fidelity. However, if tunnelling takes on a significant role then the timescale for nuclear motion $\overline{\nu}$ no longer depicts the speed at which a molecule can be switched. Tunnelling reactions proceed much slower than barrierless, classically allowed, activated reactions occurring at the critical field strength, with the reaction rate decreasing exponentially with increasing energy saving. Hence the ability of quantum nuclear tunnelling to aid the *classical* processes depicting basic QCA operation is strictly limited. This reality is starkly different to naïve expectations that tunnelling would aid molecular QCA operation by possibly reducing power dissipation to nearly zero;[7, 9-11, 35] under such circumstances, the fidelity of "0" to "1", "0" to "null", etc. transitions also becomes zero.

How this works out in practice can be gauged from the results of the quantum simulations of Blair et al..[40] For this nearly optimal example of power reduction by tunnelling, the reduction factor is about 5, but the required tunnelling rate means essentially no latching, with a fidelity of just 95% if the field is maintained at the minimum value required for switching. Further, the system discussed presents the mutually inconsistent scenario of demanding slow change of the external field to a molecular switch, but then using molecular switches to provide the field to nearby molecular switches, ensuring that the applied field switches at the same rate as the tunnelling.

Conclusions

Taking results predicted for the iconic 1,4-diallyl cation by different computational methods as paradigms for the operation of molecular electronic devices, we see that the much-discussed scenario, involving use of intervalence systems as bistable molecular switches in logic devices such as QCA cells, leads inevitably to significant power dissipation, but that this facilitates internal latching to enable operation of large integrated circuits. Additionally, we see that because of their large electronic polarizability, delocalized intervalence systems act as classical dielectrics to provide useful functionality in QCA circuits without internal energy dissipation; however, they provide no internal latching.

The strong-tunnelling scenario depicted by Blair et al.[40] depicts a realizable situation intermediary between the above two classical descriptions of molecular switching, considering a bistable switch that only supports a few vibrational quantum levels in each of its potential wells. This could reduce power dissipation if some scenario could be engineered in which the fast switching of one component produces only slowly changing fields at the inputs to a connected component, but does so at the expense of latch minimization. Engineering such a scenario would have the advantage over a delocalized mixed-valence system in that nuclear polarization could be used to enhance electronic polarization and hence make a more pronounced switching effect, brought about at the expense of increased power dissipation.

In any digital electronic circuit, some form of latching will always be required, and the energy cost, assuming each and every part of the circuit supports internal latching, is not unreasonable for the development of large-scale integrated devices with functionality comparable to those currently fabricated using only silicon-based technologies. Nevertheless, mixing of passive elements, based on delocalized mixed-valence with active ones based on bistable switches, could provide sufficient latching at reduced power demands. Alternatively, cells based on delcoalized systems could be latched purely through system architecture.[35, 36]

6-site QCA cells (Fig. 1) provide a useful starting point for technology as they are driven not only by changing signals on their "input" lines, but also by clocking pulses applied to control their "null" state. Within integrated circuits, these clocking pulses can be provided down conductive busses, and all power needed to operate bistable switch molecules or to latch cells made from monostable molecules can be drawn from the clocking pulses.[36] This makes for feasible electrical engineering design.

The traditionally used label "Quantum Cellular Automata" for these devices was coined based on the assumption that quantum nuclear tunnelling would take a significant role in reducing energy demands below those demanded for classical chemical reactions occurring on Born-Oppenheimer potential-energy surfaces, as is demonstrated in the results recently

presented by Blair et al..[40] However, we show that molecules may indeed be more useful in QCA cells if the cell operation exploits only classical chemical dynamics.

Methods

UHF calculations were performed using Gaussian-09[70] mostly with the STO-3G basis set,[71] but results obtained using 6-31G*[72] instead showed little difference; the lack of qualitative difference of results for this system on basis set have also previously been noted.[6] Calculations are also performed using the 6-31G* basis by B3LYP[73] and CAM-B3LYP.[74, 75] CASSCF and MRCI calculations are performed using MOLPRO[76] with the 6-31G* basis.

Conflicts of interest

The authors note there are no conflicts to declare.

Acknowledgements

We thank the Chinese National Science Foundation for support through grant 1167040630.

1 Notes and references
2 B. Razavi, *Design of Analog CMOS Integrated Circuits*, McGraw-Hill, New York, 2016.
3 A. Aviram and M. A. Ratner, *Chem. Phys. Letts.*, 1974, **29**, 277.
4 A. Aviram, *J. Am. Chem. Soc.*, 1988, **110**, 5687.
5 R. Kubo and Y. Toyozawa, *Prog. Theor. Phys.*, 1955, **13**, 160.
6 N. S. Hush, *J. Chem. Phys.*, 1958, **28**, 962.
7 N. S. Hush, A. T. Wong, G. B. Bacskay and J. R. Reimers, *J. Am. Chem. Soc.*, 1990, **112**, 4192.
8 C. S. Lent, P. D. Tougaw, W. Porod and G. H. Bernstein, *Nanotechnology*, 1993, **4**, 49.
9 C. S. Lent and P. D. Tougaw, *Proceedings of the Ieee*, 1997, **85**, 541.
10 C. S. Lent, *Science*, 2000, **288**, 1597.
11 C. S. Lent, B. Isaksen and M. Lieberman, *J. Am. Chem. Soc.*, 2003, **125**, 1056.
12 C. S. Lent, M. Liu and Y. Lu, *Nanotechnology*, 2006, **17**, 4240.
13 J. Y. Jiao, G. J. Long, F. Grandjean, A. M. Beatty and T. P. Fehlner, *J. Am. Chem. Soc.*, 2003, **125**, 7522.
14 Z. Li, A. M. Beatty and T. P. Fehlner, *Inorg. Chem.*, 2003, **42**, 5707.
15 Z. Li and T. P. Fehlner, *Inorg. Chem.*, 2003, **42**, 5715.
16 H. Qi, S. Sharma, Z. Li, G. L. Snider, A. O. Orlov, C. S. Lent and T. P. Fehlner, *J. Am. Chem. Soc.*, 2003, **125**, 15250.
17 Y. L. Wang and M. Lieberman, *Ieee Transactions on Nanotechnology*, 2004, **3**, 368.
18 Y. Lu and C. S. Lent, *Journal of Computational Electronics*, 2005, **4**, 115.
19 W. Hu, K. Sarveswaran, M. Lieberman and G. H. Bernstein, *IEEE Transactions on Nanotechnology*, 2005, **4**, 312.
20 A. S. Bonilla, R. Gutierrez, L. M. Sandonas, D. Nozaki, A. P. Bramanti and G. Cuniberti, *Phys. Chem. Chem. Phys.*, 2014, **16**, 17777.
21 Y. Lu and C. S. Lent, *Nanotechnology*, 2008, **19**.
22 E. Rahimi and S. M. Nejad, *7th IEEE Int Conf on Communication Systems Networks and Digital Signal Processing*, 2010, 347.
23 K. Tokunaga, *Materials*, 2010, **3**, 4277.
24 Y. Lu and C. Lent, *Phys. Chem. Chem. Phys.*, 2011, **13**, 14928.
25 X. Wang and J. Ma, *Phys. Chem. Chem. Phys.*, 2011, **13**, 16134.
26 E. Rahimi and S. M. Nejad, *Nanoscale Research Letters*, 2012, **7**.
27 K. F. Albrecht, H. Wang, L. Muehlbacher, M. Thoss and A. Komnik, *Phys. Rev. B*, 2012, **86**.
28 E. Rahimi and S. M. Nejad, *Mol. Phys.*, 2013, **111**, 697.
29 Y. Lu and C. S. Lent, *Chem. Phys. Lett.*, 2013, **582**, 86.
30 X. Wang, S. Chen, J. Wen and J. Ma, *The Journal of Physical Chemistry C*, 2013, **117**, 1308.
31 M. Taucer, L. Livadaru, P. G. Piva, R. Achal, H. Labidi, J. L. Pitters and R. A. Wolkow, *Physical Review Letters*, 2014, **112**, 256801.
32 A. V. Palii, J. M. Clemente-Juan, E. Coronado and B. Tsukerblat, *The Journal of Physical Chemistry C*, 2015, **119**, 7911.
33 B. Tsukerblat, A. Palii, J. M. Clemente-Juan and E. Coronado, *The Journal of Chemical Physics*, 2015, **143**, 134307.
34 A. Palii, B. Tsukerblat, J. M. Clemente-Juan and E. Coronado, *Journal of Physical Chemistry C*, 2016, **120**, 16994.
35 N. R. Erickson, C. D. Holstrom, H. M. Rhoda, G. T. Rohde, Y. V. Zatsikha, P. Galloni and V. N. Nemykin, *Inorg. Chem.*, 2017, **56**, 4716.
36 J. Timler and C. S. Lent, *J. Appl. Phys.*, 2002, **91**, 823.
37 R. K. Kummamuru, J. Timler, G. Toth, C. S. Lent, R. Ramasubramaniam, A. O. Orlov, G. H. Bernstein and G. L. Snider, *Appl. Phys. Lett.*, 2002, **81**, 1332.
38 C. S. Lent and B. Isaksen, *IEEE Trans. Electron Devices*, 2003, **50**, 1890.
39 J. Y. Jiao, G. J. Long, L. Rebbouh, F. Grandjean, A. M. Beatty and T. P. Fehlner, *J. Am. Chem. Soc.*, 2005, **127**, 17819.
40 N. S. Hush, *Prog. Inorg. Chem.*, 1967, **8**, 391.
41 E. P. Blair, S. A. Corcelli and C. S. Lent, *The Journal of Chemical Physics*, 2016, **145**, 014307.
42 R. A. Marcus, *J. Chem. Phys.*, 1956, **24**, 966.
43 V. G. Levich and R. R. Dogonadze, *Proc. Akad. Naukl. SSSR*, 1959, **29**, 9.Dokl. Akad. Nauk. SSSR Ser. Fiz. Khim. (1959) vol. 124 pages 123-126.
44 N. S. Hush, *Trans. Farad. Soc.*, 1961, **57**, 577.
45 N. S. Hush, *Chem. Phys.*, 1975, **10**, 361.
46 S. B. Piepho, E. R. Krausz and P. N. Schatz, *J. Am. Chem. Soc.*, 1978, **100**, 2996.
47 N. S. Hush, *NATO Adv. Study Inst. Ser., Ser. C*, 1980, **58**, 151.
48 J. R. Reimers and N. S. Hush, in *Mixed Valence Systems: Applications in Chemistry, Physics, and Biology*, ed. K. Prassides, Kluwer Acad. Publishers, Dordrecht, 1991, pp. 29.
49 N. S. Hush, *J. Electroanal. Chem.*, 1999, **460**, 5.
50 J. R. Reimers and N. S. Hush, *Chem. Phys.*, 2004, **299**, 79.
51 M. Taucer, F. Karim, K. Walus and R. A. Wolkow, *Ieee Transactions on Nanotechnology*, 2015, **14**, 638.
52 J. R. Reimers, L. McKemmish, R. H. McKenzie and N. S. Hush, *Phys. Chem. Chem. Phys.*, 2015, **17**, 24598.
53 L. McKemmish, R. H. McKenzie, N. S. Hush and J. R. Reimers, *Phys. Chem. Chem. Phys.*, 2015, **17**, 24666.
54 P. H. Cribb, S. Nordholm and N. S. Hush, *Chem. Phys.*, 1979, **44**, 315.
55 J. R. Reimers and N. S. Hush, *Chem. Phys.*, 1989, **134**, 323.
56 L. K. McKemmish, D. J. Kedziora, G. R. White, N. S. Hush and J. R. Reimers, *Aust. J. Chem.*, 2012, **65**, 512.
57 F. London, *Z. Phys.*, 1932, **74**, 143.
58 J. R. Reimers, L. McKemmish, R. H. McKenzie and N. S. Hush, *Phys. Chem. Chem. Phys.*, 2015, **17**, 24640.
59 U. Öpik and M. H. L. Pryce, *Proc. R. Soc. London, A*, 1957, **238**, 425.
60 J. R. Reimers and N. S. Hush, *Chem. Phys. Lett.*, 2017, **683**, 467.
61 L. K. McKemmish, R. H. McKenzie, N. S. Hush and J. R. Reimers, *J. Chem. Phys.*, 2011, **135**, 244110.

62 R. A. Marcus, *J. Chem. Phys.*, 1965, **43**, 679.
63 V. G. Levich and R. R. Dogonadze, *Proc. Akad. Naukl. SSSR*, 1960, **133**, 591.Dokl. Akad. Nauk. SSSR Ser. Fiz. Khim. (1960) vol. 133 pages 591-4.
64 J. R. Reimers and N. S. Hush, *J. Phys. Chem.*, 1991, **95**, 9773.
65 Z.-L. Cai and J. R. Reimers, *J. Chem. Phys.*, 2000, **112**, 527.
66 J. R. Reimers, A. Sajid, R. Kobayashi and M. J. Ford, *Journal of Chemical Theory and Computation*, 2018, **14**, 1602.
67 Z.-L. Cai, M. J. Crossley, J. R. Reimers, R. Kobayashi and R. D. Amos, *J. Phys. Chem. B*, 2006, **110**, 15624.
68 Z.-L. Cai, K. Sendt and J. R. Reimers, *J. Chem. Phys.*, 2002, **117**, 5543.
69 E. B. Wilson, J. C. Decius and P. C. Cross, *Molecular Vibrations: The Theory of Infrared and Raman Vibrational Spectra*, McGraw-Hill Book Company, New York, 1955.
70 J. R. Reimers, *J. Chem. Phys.*, 2001, **115**, 9103.
71 M. J. Frisch, G. W. Trucks, H. B. Schlegel and et al, *Gaussian 09, Revision D.02*, Gaussian, Inc., Pittsburgh PA, 2009.
72 W. J. Hehre, R. F. Stewart and J. A. Pople, *J. Chem. Phys.*, 1969, **51**, 2657.
73 W. J. Hehre, R. Ditchfield and J. A. Pople, *J. Chem. Phys.*, 1972, **56**, 2257.
74 A. D. Becke, *J. Chem. Phys.*, 1993, **98**, 5648.
75 T. Yanai, D. P. Tew and N. C. Handy, *Chem. Phys. Lett.*, 2004, **393**, 51.
76 R. Kobayashi and R. D. Amos, *Chem. Phys. Lett.*, 2006, **420**, 106.
77 P. J. Knowles, R. Lindh, F. R. Manby, M. Schütz and e. al, *MOLPRO, version 2010.1, a package of ab initio programs*, University of Birmingham, Birmingham, 2010.